DOI: 10.4274/jems.2023.18942

Journal of ETA Maritime Science 2023;11(3):137-147

Numerical Investigation of the Maneuvering Forces of Different DARPA Suboff Configurations for Static Drift Condition

Hasan Öztürk, Kadir Beytulllah Gündüz, Yasemin Arıkan Özden

Yıldız Technical University Faculty of Naval Architecture and Maritime, Department of Naval Architecture and Marine Engineering, İstanbul, Türkiye

Abstract

In this study, the maneuvering forces and moments of the DARPA Suboff submarine model were determined under static drift condition using computational fluid dynamics (CFD) methods. Two different configurations of the submarine model namely; the AFF-3 configuration, which consists of bare hull and four stern rudders, and the fully appended configuration AFF-8, which is formed from bare hull, sail, and four stern rudders, have been used. Initially, for the AFF-3 configuration, a mesh independence study has been conducted. Three different cases; coarse, medium and fine meshes are investigated at small angles (0-2-4-6 degrees). After that the results have been verified, the medium mesh structure has been selected and the analyzes have been continued for larger angles (from 00 to 180 degrees). The accuracy of the obtained results was assessed by comparing them with non-dimensional experimental results. The comparison between the CFD results and the experimental results demonstrated a high level of agreement, indicating the effectiveness and accuracy of the CFD methods used in this study. After the validation studies, the maneuvering forces and moments of the AFF-8 fully appended configuration were calculated for which no prior experimental data existed in the literature. To achieve this, steady-state CFD simulations were performed using the commercial software ANSYS Fluent, and the results were presented for the same flow angles.

Keywords: Submarine, Maneuvering forces, Static drift, DARPA Suboff, CFD

1. Introduction

Submarines can be designed for military, research, equipment installation, and maintenance purposes by considering many parameters during the design process. Besides many specifications of a ship, it is of great importance to evaluate its maneuvering characteristics. In the past, many studies have been conducted to estimate the maneuvering characteristics of ships and submarines with good precision. To determine the maneuvering performance of vessels, four different methods are generally used in the literature. Empirical and semi-empirical methods are generally used in the early design stages to determine the hydrodynamic properties of the vehicle. Its advantages are that necessary changes can be made quickly and at low cost. With the use of experimental methods generally the most reliable results are obtained since non-linear effects are included in the problem by their nature. With numerical methods, characteristics such as force, velocity, pressure, and turbulence can be obtained faster and cheaper than experimental methods and also in areas where it would be difficult to collect experimental data. System diagnostic methods based on statistical theory have become increasingly popular in recent years because they offer the possibility of fast results [1].

In 1989, Groves et al. [2] described the DARPA SUBOFF submarine model as a recommended submarine hull form for benchmark tests. In 1990, Roddy [3] conducted towing tank experiments to investigate stability and control characteristics. In this study, experimental results belonging to different configurations of DARPA SUBOFF are presented [3]. Detailed flow measurements are published by Huang and Liu [4] based on measurements in a wind tunnel. DARPA SUBOFF submarine models are extensively used in submarine research studies. Generally among

Address for Correspondence: Yasemin Arıkan Özden, Yıldız Technical University Faculty of Naval Architecture and Maritime, Department of Naval Architecture and Marine Engineering, İstanbul, Türkiye
E-mail: yarikan@yildiz.edu.tr
ORCID ID: orcid.org/0000-0001-9909-0859

Received: 24.11.2022
Last Revision Received: 09.05.2023
Accepted: 05.06.2023

To cite this article: H. Öztürk, K. B. Gündüz, and Y. Arıkan Özden. "Numerical Investigation of the Maneuvering Forces of Different DARPA Suboff Configurations for Static Drift Condition." *Journal of ETA Maritime Science*, vol. 11(3), pp. 137-147, 2023.

the benchmark submarines, the main reason for using the DARPA Suboff generic model is the optimized and streamlined hull form. It is also interesting to use DARPA Suboff geometry because of the many studies that can be found in the open literature. The use of the bare hull (AFF-1) and the fully appended configuration (AFF-8) are also recommended to the researchers by the ITTC-Maneuvering Committee, 2014 [5].

Toxopeus and Vaz [6] previously studied the flow at different drift angles around the bare hull of the DARPA SUBOFF configuration. They used their own code and completed the verification and validation study. In their study, different turbulence models were used and results were presented [6]. Vaz et al. [7] conducted another study to calculate the maneuvering forces of DARPA SUBOFF using CFD. This time, they used two viscous-flow solvers and focused on the accurate prediction of the maneuvering forces and moments of the DARPA SUBOFF AFF-1 and AFF-8 configurations for 0° and 18° drift angles. They investigated the influence of different turbulence models. The results obtained using Reynolds-Averaged-Navier-Stokes (RANS) approach are compared with the theoretically more realistic Delayed-Detached-Eddy-Simulation (DDES) results. They also investigated the influence of the appendages on the forces and flow fields [7]. In a collaborative CFD exercise, the Submarine Hydrodynamics Working Group, which consists of different institutions, performed calculations on the bare hull of the DARPA SUBOFF submarine to investigate the capability of RANS viscous flow solvers to predict the flow field around the hull and the forces and moments for several steady turns. The study was conducted using several different viscous flow solvers, turbulence models, and grid types. The study improved the knowledge and understanding of underwater vehicle hydrodynamics. They performed verification and validation of the solutions and in several cases the results were validated at acceptable levels (below 10%). They also stated that modeling errors are present in the cases for which validation was not achieved and these can be attributed to the turbulence model [8]. In their study, Pan et al. [9] tried to predict submarine hydrodynamic coefficients by numerical simulations. They have carried out steady and unsteady RANS simulations. They made the simulation of the oblique towing tank experiment and the planar motion mechanism (PMM) experiment performed on the SUBOFF submarine model. They explored the possibility of developing a numerical method to evaluate the maneuvering characteristics of a submarine, especially at an earlier stage of the design cycle. Consequently, the studies were verified with the experimental data, and a good agreement between each other has been seen. They also have stated that PMM experiment may be the most effective way; however, it requires special facilities and equipment and is both time-consuming and costly, and not economical at the preliminary design stage [9].

Ray and Sen [10] estimated the hydrodynamic coefficients using the System Identification (SI) technique of the Extended Kalman Filter for a submarine from its full-scale maneuvering sea trials data. Data from sea trials with two submarines were used to identify the hydrodynamic coefficients. The authors provide advice for problems related to the robustness of SI techniques applied to the identification of hydrodynamic parameters from noisy full-scale data [10]. Jiang et al. [11] performed a study on the prediction of straight-line hydrodynamic coefficients for a portable autonomous underwater vehicle using empirical methods and computational fluid dynamics (CFD). They compared empirical and CFD results with experimental results obtained from wind tunnel tests. They showed trends in the variation of forces and moments and that they can be captured well by CFD [11].

Shadlaghani and Mansoorzadeh [12] investigated the advantage of steady test simulations relative to unsteady experiments, especially PMM tests, for computing velocity-based hydrodynamic coefficients. Steady maneuvers including towing with drift and attack angles together with rotating arm tests were simulated to calculate the linear damping coefficients of DARPA Suboff. The obtained results were compared with available unsteady experimental results of the SUBOFF submarine. It was also stated that the expensive and complicated unsteady simulations of PMM maneuvers can be replaced by simple steady-state simulations by towing and rotating the model [12]. Lin et al. [13] established an efficient experimental procedure to analyze the maneuvering derivatives of a half-scale submerged body of DARPA SUBOFF in the horizontal plane for four different configurations, including bare hull, bare hull with sail, bare hull with rudders, and bare hull with all appendages. They conducted PMM experiments in the towing tank of National Cheng Kung University. The results obtained for evaluating the feasibility of the test method and verifying the results compared with the results of previous experiments performed by DTRC [13]. They also improved the design of the flange connecting the load cell with the stainless strut to reduce the installation time in the PMM tests. The results about the uncertainty of the test results are presented [13]. Atik [14] investigated a suitable solution mesh and turbulence model for the DARPA SUBOFF submarine AFF-1 hull form by performing static drift test simulations. She compared the obtained results with experimental results conducted by DTRC/SHD. She stated that all turbulence models gave close results at small angles, small differences were seen between the models

as the angles increased, and the Shear Stress Transport (SST) k-ω turbulence model gave the closest results, while after 8 degrees of static drift, there was an average of 10% difference between numerical and experimental results [14].

Kahramanoglu [15] examined the scale effects on the horizontal maneuvering derivatives for three different scales for the fully appended DARPA Suboff submarine. To achieve this, a numerical viscous solver was used to model the PMM. Pure sway and pure yaw calculations for the model scale of the DARPA Suboff were performed numerically. After the verification assessment of the numerical results, the sway forces and yaw moments are obtained for different scenarios and the linear horizontal maneuvering derivatives are obtained for different scales. The comparison revealed that the sway forces obtained from pure yaw analyzes exhibited significant sensitivity to changes in scale, whereas the sway forces obtained from pure sway analyzes were relatively insensitive. The results also indicated that neither pure sway nor pure yaw analyzes showed a significant sensitivity to changes in scale for the yaw moment values, as reported by the author [15].

This study focused on conducting maneuvering analyzes of the AFF-3 and AFF-8 configurations using CFD simulations. Specifically, the analyzes were carried out for drift angles ranging from 0 to 18 degrees at a speed of 6.5 knots. The obtained results were brought to the non-dimensional values to compare with the experimental results presented by Liu and Huang [16]. After validation of the results of the AFF-3 configuration, the same calculations are applied to the AFF-8 fully appended configuration. Due to the DARPA Suboff submarine's symmetry about the y-axis, the calculations were performed solely for the PS. The primary objective of this study is to examine the forces and moments in the static drift condition of the AFF-8 configuration, which has no available experimental data in the literature.

2. Methodology

To be able to make a better prediction about the hydrodynamic forces and moments, the six degrees of freedom maneuvering motion is decoupled into the horizontal and the vertical motions; thus, the problem can be simplified into a set of linear equations. Therefore, the estimation of the hydrodynamic coefficients of these motion equations is a key step in predicting the motion of the submarine.

2.1. Maneuvering Equations

The generalized 6-DoF rigid-body equations of motion in a body-fixed, non-inertial frame of reference XYZ that is moving relative to an Earth-fixed, inertial reference frame $X_0 Y_0 Z_0$ can be derived as follows [17]:

$$m\left[\dot{u}-vr+\omega q-x_G\left(q^2+r^2\right)+y_G\left(pq-\dot{r}\right)+z_G\left(pr+\dot{q}\right)\right]=X \quad (1)$$

$$m\left[\dot{v}-\omega p+ur-y_G\left(r^2+p^2\right)+z_G\left(qr-\dot{p}\right)+x_G\left(qp+\dot{r}\right)\right]=Y \quad (2)$$

$$m\left[\dot{\omega}-uq+vp-z_G\left(p^2+q^2\right)+x_G\left(rp-\dot{q}\right)+y_G\left(rq+\dot{p}\right)\right]=Z \quad (3)$$

$$I_x\dot{p}+\left(I_z-I_y\right)qr-\left(\dot{r}+pq\right)I_{xz}+\left(r^2-q^2\right)I_{yz}+\left(pr-\dot{q}\right)I_{xy}+m\left[y_G\left(\dot{\omega}-uq+vp\right)-z_G\left(\dot{v}-\omega p+ur\right)\right]=K \quad (4)$$

$$I_y\dot{q}+\left(I_x-I_z\right)rp-\left(\dot{p}+qr\right)I_{xy}+\left(p^2-r^2\right)I_{zx}+\left(qp-\dot{r}\right)I_{yz}+m\left[z_G\left(\dot{u}-vr+\omega q\right)-x_G\left(\dot{\omega}-uq+vp\right)\right]=M \quad (5)$$

$$I_z\dot{r}+\left(I_y-I_x\right)pq-\left(\dot{q}+rp\right)I_{yz}+\left(q^2-p^2\right)I_{xy}+\left(rq-\dot{p}\right)I_{zx}+m\left[x_G\left(\dot{v}-\omega p+ur\right)-y_G\left(\dot{u}-vr+\omega q\right)\right]=N \quad (6)$$

Equations 1, 2, and 3 represent the translational motions; surge-x, sway-y, and heave-z, and 4, 5 and 6 represent the rotational motions; roll-ϕ, pitch-θ and yaw-ψ, respectively. These given 6-DoF equations of motion represent the forces and moments; X, Y, Z which are the external forces acting on the submarine and K, M, N are the external moments, respectively. In maneuvering studies two coordinate systems are used; an inertial coordinate system (or fixed on earth x_0-y_0-z_0) and a moving coordinate system (or fixed on body x-y-z). Also, m describes the mass of the vessel and I_X, I_Y, I_Z are the moments of inertia of the vessel for each axis. In the equations the points (x_G, y_G, z_G) define the center of gravity of the submarine. In this study, the coordinate system is used so that the longitudinal axis of the submarine is in the x-axis and the bow is in the positive x direction, the y-axis is positioned to determine the starboard (SB) and PS of the submarine, and the z-axis is positioned vertically upwards to the submarine (Figure 1). The position of the center of moment used in moment calculations on the z-axis is determined according to the center of gravity of the model at 0.4621*Loa distance from the stern.

$$\left\{\begin{array}{ll}\dot{x}=u & \rightarrow\text{surge velocity}\\ \dot{y}=v & \rightarrow\text{sway velocity}\\ \dot{z}=\omega & \rightarrow\text{heave velocity}\end{array}\right\}\xrightarrow{\frac{d}{dt}}\left\{\begin{array}{ll}\ddot{x}=\dot{u} & \rightarrow\text{surge acceleration}\\ \ddot{y}=\dot{v} & \rightarrow\text{sway acceleration}\\ \ddot{z}=\dot{\omega} & \rightarrow\text{heave acceleration}\end{array}\right\}$$

The rotational velocities and accelerations are given below for each axis:

$$\left\{\begin{array}{ll}\dot{\phi}=p & \rightarrow\text{roll rate}\\ \dot{\theta}=q & \rightarrow\text{pitch rate}\\ \dot{\psi}=r & \rightarrow\text{yaw rate}\end{array}\right\}\xrightarrow{\frac{d}{dt}}\left\{\begin{array}{ll}\ddot{\phi}=\dot{p} & \rightarrow\text{roll acceleration}\\ \ddot{\theta}=\dot{q} & \rightarrow\text{pitch acceleration}\\ \ddot{\psi}=\dot{r} & \rightarrow\text{yaw acceleration}\end{array}\right\}$$

For submarines and ships, forces and moments acting on the hull are in the horizontal plane. In this case, the heave, pitch, and roll motions are neglected; in other words, these values become $\omega = p = q = \dot{\omega} = \dot{p} = \dot{q} = 0$. In the XZ plane $y_G = 0$ because of the symmetry of the submarine. If we apply these simplifications to the equations of motion,

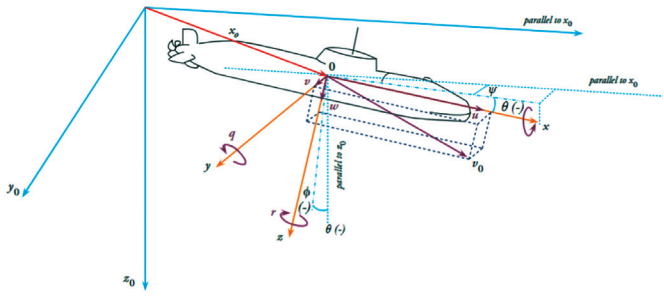

Figure 1. *Fixed and moving reference frames of a submarine [18]*

the aforementioned equations become as shown in the Equations (7), (8) and (9) respectively for surge, sway, and yaw. If we look at past studies to better understand the maneuvering ability of vessels, some studies can be found. One of the most preferred studies belongs to Abkowitz [19], who proposed a model based on solving the equations of motion for the hydrodynamic forces (X, Y) and moment (N) acting on the hull by considering the ship as a whole, and based on the expansion of hydrodynamic forces (X, Y) and moment (N) to the third-order Taylor series [19]. Yoon [20] studied Abkowitz's [19] maneuvering model in his PhD thesis and obtained hydrodynamic derivatives of the surface combatant model DTMB5415 by conducting PMM tests.

$$m\left(\dot{u} - vr - x_G r^2\right) = X \tag{7}$$

[[OMML-EQ-3]] (8)

$$I_z \dot{r} + m x_G(\dot{v} + ur) = N \tag{9}$$

Velocity coordinates are V = (u, v, w). Here, u defines the velocity on the x-axis and v defines the velocity on the y-axis. U and V velocities occur because of the β static drift angle. All integral forces and moments on the hull are based on a right-handed axis system that corresponds to the positive directions normally applied in maneuvering operations. This means that the X force directs Y to the SB and Z downwards. To be able to compare with the experimental results obtained values should be nondimensionalized. It should also be known that the hydrodynamic derivatives used in ship-maneuvering studies are commonly known as maneuvering coefficients.

2.2. The RANS Equations

RANS equations are employed to numerically solve the flow around the DARPA Suboff configurations. The governing equations are the continuity equation and the momentum equation. The continuity equation in cartesian coordinates can be given as (Equation 10):

$$\frac{\partial U_i}{\partial x_i} = 0 \tag{10}$$

The momentum equation can be written as in equation 11:

$$\frac{\partial U_i}{\partial t} + \frac{\partial (U_i U_j)}{\partial x_j} = -\frac{1}{\rho}\frac{\partial P}{\partial x_i} + \frac{\partial}{\partial x_j}\left[\nu\left(\frac{\partial U_i}{\partial x_j} + \frac{\partial U_j}{\partial x_i}\right)\right] - \frac{\partial \overline{u_i' u_j'}}{\partial x_j} \tag{11}$$

Where U_i and U_j are the mean velocity and the turbulence components, p is the mean pressure, ρ is the density, and ν is the molecular kinematic viscosity of the fluid. Since all analyses were performed at steady state for this study, the initial term was not taken into account. The k-ω turbulence model is applied in order to simulate the turbulent flow around the submarine. Because submarines are submerged bodies, there are no free surface effects. During the analyses, the Reynolds stress tensor was calculated according to the following equation.

$$\overline{u_i' u_j'} = -\nu_t\left(\frac{\partial U_i}{\partial x_j} + \frac{\partial U_j}{\partial x_i}\right) + \frac{2}{3}\delta_{ij} k \tag{12}$$

Here ν_t is the eddy viscosity and it must be modeled in order to take into account the turbulence contribution of the motion equation. It is known that various turbulence models are developed for this purpose.

2.3. Presentation of Forces and Moments

In order to be able to convert the obtained forces and moments to non-dimensional values, the following equations (Equations 13-14) are used according to the proposal of SNAME 1950 [21]. The resistive forces in the X, Y, and Z axis are non-dimensionalized by using the following formula.

$$X', Y', Z' = \frac{X, Y, Z}{\frac{1}{2}\rho V_0^2 L_{PP}^2} \tag{13}$$

K, M, N are the moments that occur around the X, Y, Z axis, respectively. To make non-dimensionalisation of these moments, the following formula is used.

$$K', M', N' = \frac{K, M, N}{\frac{1}{2}\rho V_0^2 L_{PP}^3} \tag{14}$$

The non-dimensionalisation of the maneuvering forces and moments is carried out according to Equations 13 and 14. The obtained numerical results were compared with the experimental values of the DARPA Suboff experiments [16].

3. Geometry of Bodies

The DARPA Submarine Technology Program provides resources to help develop submarines. Various experiments were carried out using the submarine model defined as the DARPA Suboff. The purpose of these experiments is to contribute to the development of submarines produced today and to be produced in the future. The SUBOFF project provides data for the CFD community to compare numerical data. Within the scope of the results given by this project, analyzes were performed on AFF-3 (Body and control surfaces) and AFF-8 (Fully appended) configurations.

The DARPA SUBOFF is a generic submarine model geometry with a length of 4.356 m and a maximum diameter of 0.508 m. According to the arrangement of the sails, rudders, and ring wings, there are different configurations of the submarine model. The stability and control characteristics of the DARPA SUBOFF model were determined experimentally for five different configurations of the DARPA Suboff submarine model in the horizontal plane and for one configuration in the vertical plane [3]. The AFF-8 configuration consists of a sail located at the top dead center of the hull starting at x=0.92 m from the bow and ending at x=1.29 m. The AFF-3 configuration has no sail. In both configurations, the cross-shaped rudders and hydroplanes are located at x=4 m from the bow. The hull and appendage arrangement of the AFF-3 and AFF-8 configurations are shown in Figure 2 and the main particulars are given in Table 1 [2].

4. Mesh Independence Study

In the present study, three different mesh sizes were used in the mesh independence study. Firstly, CFD analyzes were carried out for DARPA Suboff AFF-3 configuration. This configuration is formed from the bare hull and rudder fins. The CFD calculations were performed using a commercial finite volume method with the commercial code ANSYS Fluent. Steady-state RANS simulations were conducted for all calculations. The mesh generation was carried out using both structured and unstructured mesh techniques in Pointwise. The submarine model was investigated in a spherical computational domain with a radius of approximately eight times its own length. The total grid number is nearly $16x10^6$ elements (Figure 3). T-REX elements were used to provide the non-dimensional wall distance y+≈50. A mesh independence study was conducted to select an adequate grid size with three different mesh densities: coarse, medium, and fine (Figure 4). Generally, in the mesh independence study, the growing factor is used as the mesh refinement factor. Thus, the total cell numbers that make up the entire calculation area can be changed. According to the ITTC Guidelines, this growing factor should be between $\sqrt{2}$ and 2. Also, ITTC have stated that refinement ratio r=2 may often be too large, instead of this as an alternative refinement ratio may be r=$\sqrt{2}$ [22]. The equations are discretized using a limited volume approach with cell-centered collographic variables. In the analysis of submarine models, as a solver, the ANSYS-Fluent program based on Reynolds-Averaged-Navier-Stokes Equations, which works with the principle of the finite volume method have been used.

A spherical domain was chosen as the outer domain and its radius was determined to be eight submarine lengths. After the meshing process was completed, the surfaces were defined and CFD simulations were initiated. Since it is known that submarine models will be subject to turbulent flow, the realizable k-omega turbulence model was chosen. The reason for choosing this turbulence model is that the objects analyzed in naval engineering problems have a

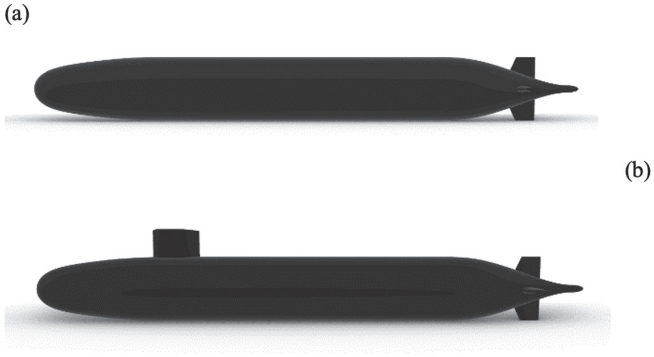

Figure 2. *Geometry of DARPA Suboff AFF-3 (a) and AFF-8 (b)*

Table 1. *Main particulars of the DARPA Suboff AFF-3 and AFF-8 models [2]*

	Symbol	Magnitude (AFF-3)	Magnitude (AFF-8)
Length overall	L_{OA}	4.356	4.356
Length between perpendiculars	L_{BP}	4.261	4.261
Maximum hull radius	R_{MAX}	0,254	0.254
Centre of buoyancy (aft of nose)	LCB	0.4625 L_{OA}	0.4621 L_{OA}
Volume of displacement		0.701	0.718
Wetted surface area	S_{WA}	6.188	6.338

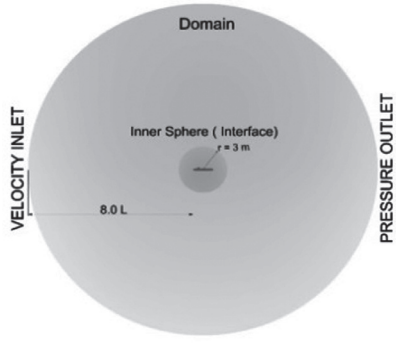

Figure 3. *Computational domain and boundary conditions*

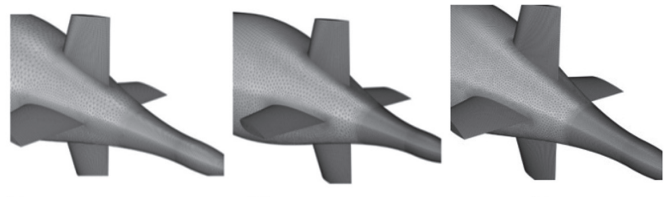

Figure 4. *Structures of Coarse (a), Medium (b) and Fine (c)*

relatively delicate structure, and this turbulence model is a good representation of the turbulent flow around such objects.

Boundary conditions can be analyzed in three parts.

- Inlet: It is determined as a speed input where the flow enters and moves forward.

- Output (Outlet): It is determined as the pressure output. By accepting the pressure value at the outlet as zero, it provides the energy conservation equation.

- Model (Wall): The Suboff model is defined as wall, so the flow cannot pass through it, and velocity and pressure changes can be observed here.

In the first part of the validation, the forces and moments for the static drift condition of the AFF-3 configuration were obtained for the model velocity V=3.3436 m/s at inflow angles changing at two-degree intervals from 0 to 6 degrees for each mesh density. Then, the CFD results were converted to non-dimensional values to be able to compare with experimental results. Medium mesh density was selected for further analysis. The analysis for larger angles were continued (at two-degree intervals from 0° to 18°) and the obtained values were compared by non-dimensional values and shown that they agree well with the experimental data.

The solution scheme is selected as Semi Implicit Methods for Pressure Linked Equations-SIMPLE and the gradient discretization is Green-Gauss node based. In the study as turbulence model SST k-ω turbulence model was selected. The spatial discretization for the pressure gradient and momentum gradient is the second order, and for the turbulent kinetic energy and specific dissipation rate, it is selected as quick. Incoming flow is defined as the velocity inlet and the outflow is defined as the pressure outlet. The turbulence intensity and viscosity ratio were selected in the boundary conditions as 2 and 5. In this process, to get better results two spheres have been used around the submarine model, where the inner domain is defined as non-slip wall and the outer spherical domain is defined as symmetry.

Table 2 shows the first validation part of the present study. As can be seen, the computational results are in very good agreement with the experimental results. Considering these results, the medium grid size was chosen to be used for further analysis. The numerical analyzes were conducted using k-ω SST turbulence model throughout all analyses. Figures 5-7 show the comparison of the CFD results with the experimental results for the AFF-3 configuration for the longitudinal force X', transverse force Y' and yawing moment N' values, respectively. The results for three different mesh densities are presented.

5. Obtaining the Maneuvering Forces and Moments for Larger Drift Angles for AFF-3 and

Table 2. *Results of the maneuvering forces and moments of the AFF-3 configuration for different mesh densities*

β=0 degree		**CFD results**			**% Errors (acc. to experiment results)**		
Grid size	Cell Number	X (N)	Y (N)	N (Nm)	(X')	(Y')	(N')
Fine	26034561	112.1016	0.0988	0.1154	1.8578	-	-
Medium	16146445	112.3571	0.0664	0.1113	1.6341	-	-
Coarse	9256715	113.1616	0.3080	0.4964	0.9298	-	-
β=2 degree		CFD results			% Errors (acc. to experiment results)		
Grid size	Cell Number	X (N)	Y (N)	N (Nm)	(X')	(Y')	(N')
Fine	26034561	111.2394	36.2315	164.2729	2.9568	6.7429	-0.1455
Medium	16146445	111.3642	34.9620	164.2448	2.8480	10.0107	-0.1284
Coarse	9256715	112.0950	34.2674	163.0828	2.2105	11.7984	0.5800
β=4 degree		CFD results			% Errors (acc. to experiment results)		
Grid size	Cell Number	X (N)	Y (N)	N (Nm)	(X')	(Y')	(N')
Fine	26034561	110.8821	81.6928	322.7482	3.5244	2.8037	5.4054
Medium	16146445	111.0518	80.2730	323.7442	3.3767	4.4930	5.1135
Coarse	9256715	111.5469	79.0410	321.7783	2.9460	5.9588	5.6897
β=6 degree		CFD results			% Errors (acc. to experiment results)		
Grid size	Cell Number	X (N)	Y (N)	N (Nm)	(X')	(Y')	(N')
Fine	26034561	110.0291	138.0959	464.8401	3.3723	5.3701	2.6802
Medium	16146445	110.2680	137.3063	466.0138	3.1624	5.9112	2.4344
Coarse	9256715	110.9607	136.2890	464.9756	2.5541	6.6083	2.6518

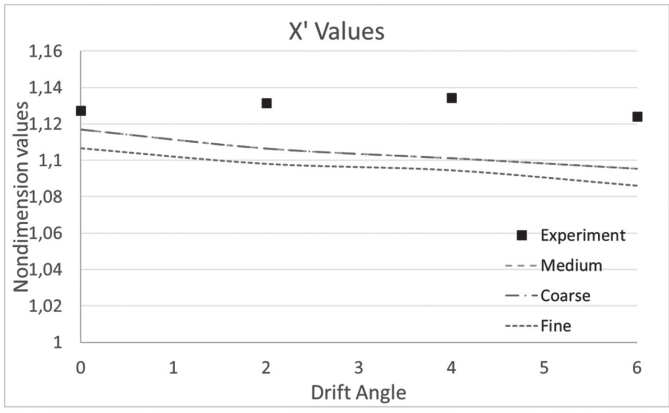

Figure 5. *Longitudinal Force X' for drift angle from 0 to 6 degrees for AFF-3 configuration*

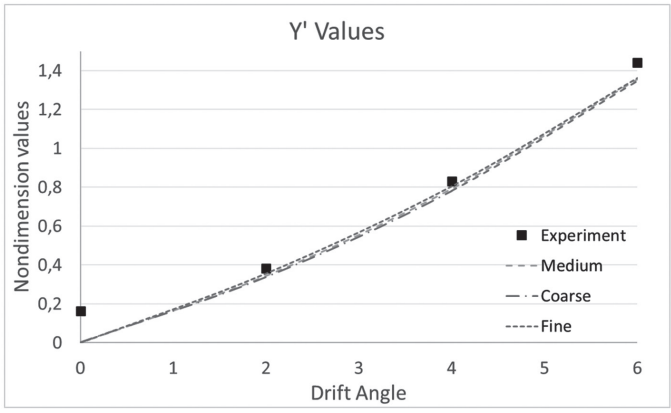

Figure 6. *Transverse Force Y' for drift angle from 0 to 6 degrees for AFF-3 configuration*

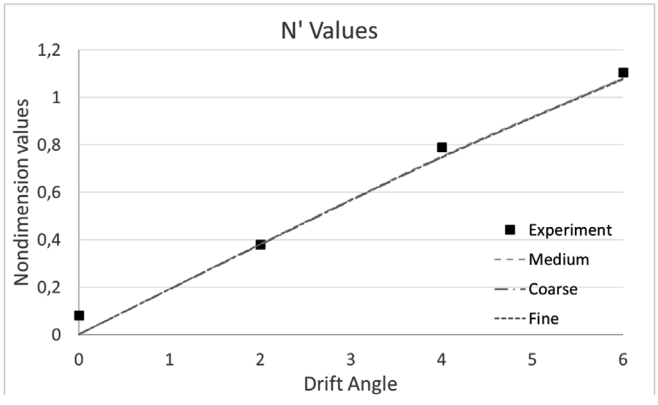

Figure 7. *Yawing Moment N' for drift angle from 0 to 6 degrees for AFF-3 configuration*

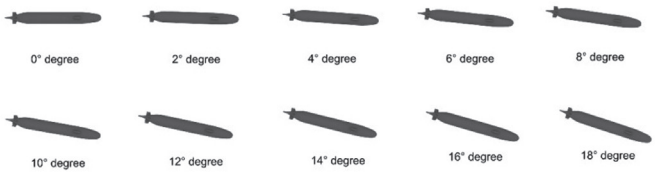

Figure 8. *The position of AFF-3 configuration at different drift angles*

AFF-8 Configuration

After selecting the medium grid size, numerical analyzes were performed at two-degree intervals from 0° to 18° for the AFF-3 configuration (Figure 8). The obtained hydrodynamic forces and moments were converted to non-dimensional values according to equations 10 and 11 as recommended by SNAME, 1950. Following, similar analyses were conducted for the fully appended AFF-8 configuration, which includes bare hull, sail, and four rudders. However, the AFF-8 configuration is extensively used in CFD validation studies and no experimental data is available for the static drift condition; therefore, it is not possible to make a comparison with experimental results. For the static drift condition, a numerical result found only for 18° was used for comparison [6].

The obtained values for the AFF-3 configuration from 0 to 18 degrees are compared with experimental data and are shown in Figures 9-11 and the calculation results obtained are given in Table 3.

From the figures it is seen that the results are in good

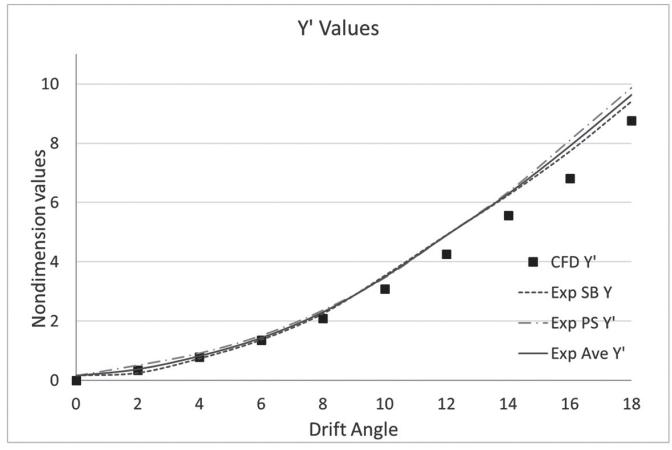

Figure 9. *Longitudinal Force X' for drift angle from 0 to 18 degrees for AFF-3 configuration*

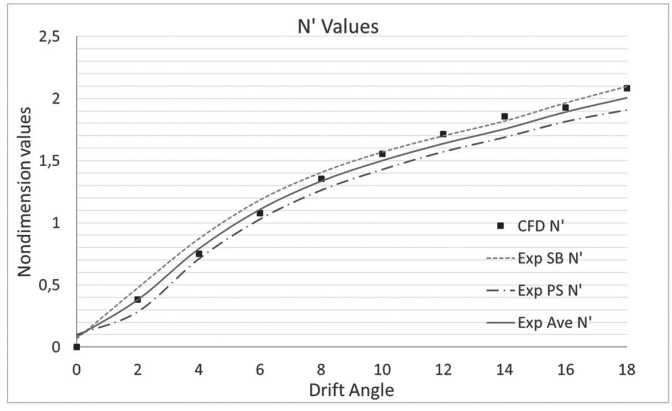

Figure 10. *Transverse Force Y' for drift angle from 0 to 18 degrees for AFF-3 configuration*

agreement with the experimental results. The experimental results are given for the incoming flow coming from both sides, namely the SB and PS. These two experimental results can be interpreted as the uncertainty of the experiments. It is seen that the CFD results are in the vicinity of the two experimental results. The deviation rates comparing the values obtained from CFD and experimental results are shown in Table 4.

After the studies for the AFF-3 configuration, analyses were run for the AFF-8 configuration using the same mesh structure and boundary conditions. The analysis results obtained by CFD are shown in Table 5. The CFD results obtained for 18 degrees are compared with the results obtained by Toxopeus et al. [7] and it is seen that the results are in good agreement. Toxopeus et al. [8] presented the longitudinal force X' as 0.85, transverse force Y' as 11.866, and the yawing moment N' as 2.973 for the static drift angle 18 degrees. The benchmark graphics are shown in Figures 12-14.

After the validation studies, the results for both configurations are compared. From Figure 15 to Figure 17, the results for the AFF-3 and AFF-8 configurations are given for the longitudinal force X', transverse force Y' and yawing moment N' for the drift angles from 0 to 18 degrees in comparison. The AFF-3 configuration is formed from bare hull and four stern rudders. In addition, the AFF-8 configuration has a sail in the location at the top dead center of the hull starting from the bow at x=0.92 m and ending at x=1.29 m. The difference between the two configurations can be interpreted as the effect of the sail on the forces and moments. In the longitudinal force, an irregularity is seen for the drift angles 9-18 degrees. An increase in the transverse forces and yawing moments are seen compared with the AFF-3 configuration. Approximately at 17 degrees drift angle, the values reach their maximum value.

6. Conclusion

In the present study, forces and moments in the horizontal plane are investigated numerically for the model geometry of a benchmark submarine, DARPA Suboff AFF-3, and AFF-8 configuration using a viscous solver based on the finite volume method. First, the validation of the CFD calculations was carried out for small drift angles (from 0 to 6 degree), for the AFF-3 configuration, for which experimental data are available in the literature. To find the optimum grid size, a mesh independence study was done for three different cases; coarse, medium and fine cases at small angles (0-2-4-6 degrees) on the AFF-3 configuration and continued by selecting the medium mesh structure. Hence, the other analyzes are continued at two-degree intervals for larger angles (from 0° to 18° degrees). The results were verified and validated with available experimental data. The results of this analysis were converted into non-dimensional values and a good agreement was observed with the experimental data.

After the validation study, the analyzes of the DARPA Suboff AFF-8 configuration were carried out at two-degree

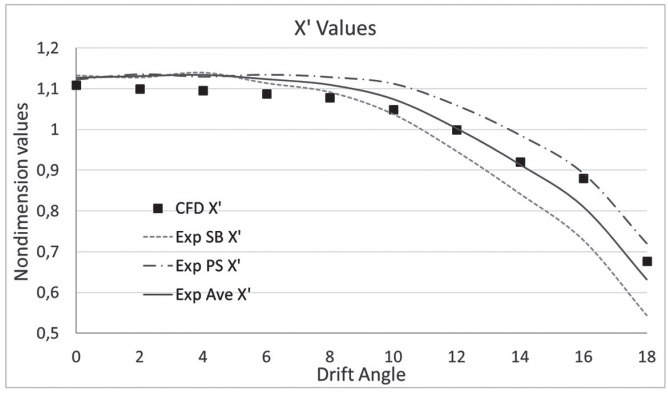

Figure 11. *Yawing Moment N' for drift angle from 0 to 18 degrees for AFF-3 configuration*

Table 3. *Result of AFF-3*

Drift angle	X (N)	X' (x10^{-3})	Y (N)	Y' (x10^{-3})	N (Nm)	N' (x10^{-3})
0	112.3570	-1.1090	-0.0664	-0.000655	0.1113	0.0002578
2	111.3641	-1.0992	-34.9619	-0.345109	164.2448	0.3804878
4	111.0517	-1.0961	-80.2729	-0.792373	323.7442	0.7499826
6	110.2680	-1.0884	-137.3062	-1.355348	466.0138	1.0795630
8	109.2802	-1.0787	-212.1415	-2.094047	585.3134	1.3559312
10	106.2250	-1.0485	-312.6999	-3.086657	672.1073	1.5569972
12	101.2737	-0.9996	-431.0689	-4.255077	740.1920	1.7147214
14	93.2992	-0.9209	-564.1457	-5.568676	801.4047	1.8565262
16	89.12992	-0.8798	-691.3075	-6.823889	831.3774	1.9259606
18	68.5620	-0.6767	-887.8658	-8.764114	899.7069	2.0842521

intervals from 0 degree to 18 degrees with the resultant speed of 3,3436 m/s. However, it should be noted that unlike other configurations, there is no available experimental data for the static drift condition of the DARPA Suboff AFF-8 configuration. Thus, a comparison with experimental results was not possible for the static drift condition of the AFF-8 configuration. Only a numerical study on the results of the AFF-8 configuration for static drift at 18 degrees is available for comparison. It has been demonstrated that the CFD results obtained for a drift angle of 18 degrees exhibit good agreement with the results presented by Vaz et al. [7], which is the only source available for comparison with AFF-8 configuration.

As a result, the forces and moments generated under static drift conditions at different angles, which were previously not available in the literature, have been added to the literature and presented in this study. The study reveals that flow separation becomes significant at large angles, and with the increasing drift angle, the forces in the X direction decrease, the forces in the Y direction increase, and the moment around the Z axis increases. The difference between the AFF-3 and AFF-8 configurations is the sail added on the top of the submarine geometry. The increase in the transverse forces and yawing moment for the AFF-8 configuration shows the effect of the sail on the static drift performance of the submarine. In future work, analyzes

Table 4. *The deviation of the AFF-3 CFD results from experimental results*

Drift angle	% Deviation (X')	% Deviation (Y')	% Deviation (N')
2	2.8480	10.0106	-0.1283
4	3.376	4.4929	5.1135
6	3.1623	5.9112	2.4344
8	2.8194	9.3486	-1.6821
10	2.4607	11.7467	-3.8690
12	0.3317	13.1882	-4.8118
14	-0.7170	11.6153	-5.9056
16	-8.5436	13.7744	-1.9026
18	-7.0001	9.1000	-4.0565

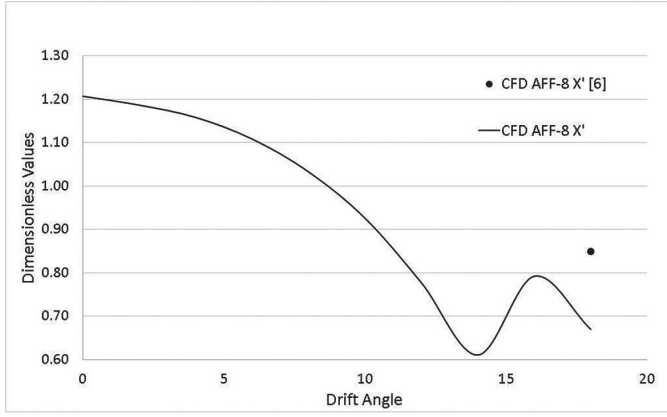

Figure 12. *Longitudinal Force X' for drift angle from 0 to 18 degrees for AFF-8 configuration*

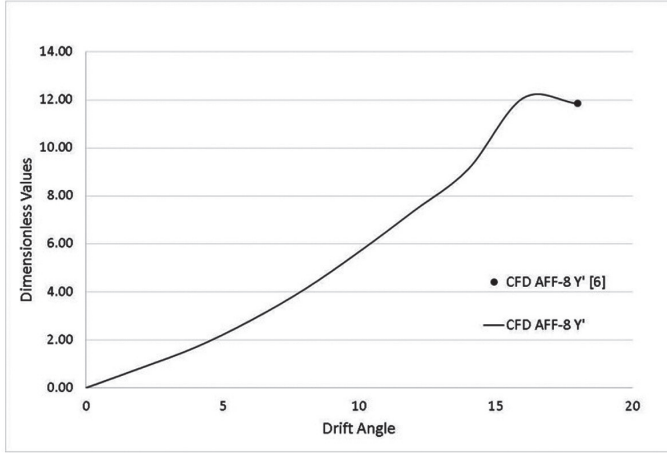

Figure 13. *Transverse Force Y' for drift angle from 0 to 18 degrees for AFF-8 configuration*

Table 5. *Forces and moments obtained by CFD for the AFF-8 configuration*

Drift angle	X (N)	X' (x10^{-3})	Y	Y' (x10^{-3})	N	N' (x10^{-3})
0	122,2605	-1,20683	-0,07076	-0,00069	0,36253	0,00084
2	120,1928	-1,18642	-83,65574	-0,82576	196,39776	0,45497
4	117,3173	-1,15803	-170,72788	-1,68525	413,57488	0,95808
6	112,2693	-1,10821	-282,83820	-2,79189	605,27235	1,40216
8	104,6136	-1,03264	-415,85953	-4,10494	780,27290	1,80757
10	93,7995	-0,92589	-574,71143	-5,67297	933,66604	2,16292
12	78,7258	-0,77710	-746,74898	-7,37115	1065,71360	2,46882
14	61,8646	-0,61066	-924,11950	-9,12197	1174,60530	2,72107
16	80,2412	-0,79206	-1223,29300	-12,07511	1298,31590	3,00766
18	67,8632	-0,66987	-1200,20900	-11,84725	1259,51750	2,91778

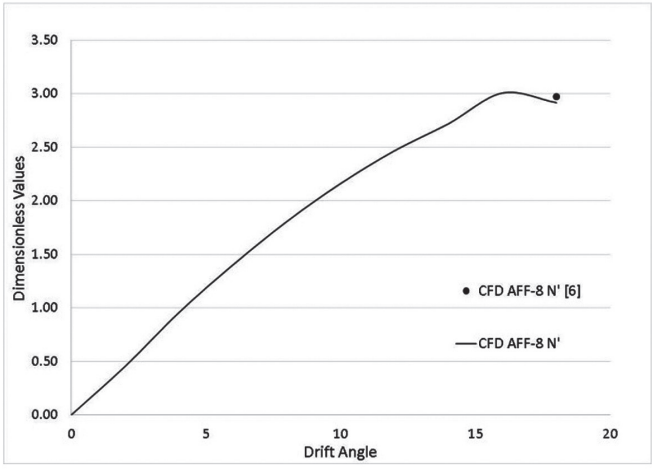

Figure 14. *Yawing Moment N' for AFF-3 and AFF-8 configurations*

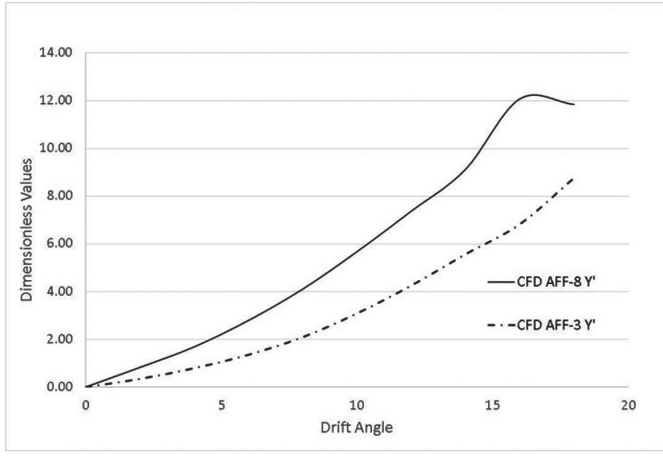

Figure 16. *Transverse Force Y' for AFF-3 and AFF-8 configurations*

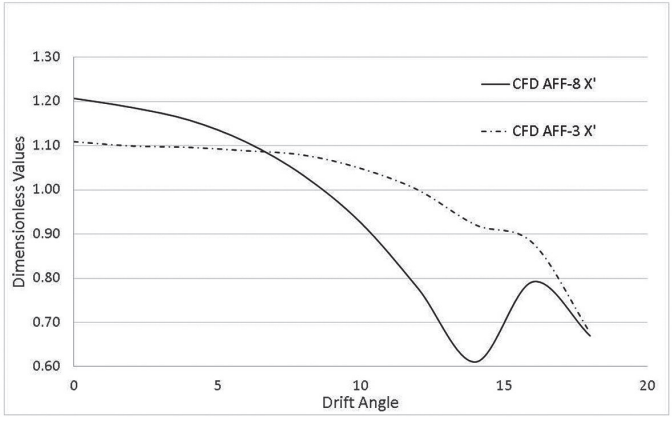

Figure 15. *Longitudinal Force X' for AFF-3 and AFF-8 configurations*

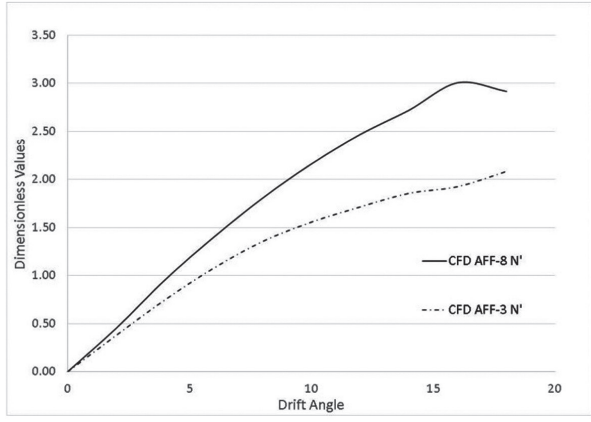

Figure 17. *Yawing Moment N' for AFF-3 and AFF-8 configurations*

will be performed with the self-propelled AFF-3 and self-propelled AFF-8 configurations on horizontal planes to see the change of forces and moments in static drift conditions.

Peer-review: Externally peer-reviewed.

Authorship Contributions

Concept design: H. Öztürk, K. B. Gündüz, Y. Arıkan Özden, Data Collection or Processing: H. Öztürk, K. B. Gündüz, Y. Arıkan Özden, Analysis or Interpretation: H. Öztürk, K. B. Gündüz, Y. Arıkan Özden, Literature Review: H. Öztürk, K. B. Gündüz, Y. Arıkan Özden, Writing, Reviewing and Editing: H. Öztürk, K. B. Gündüz, Y. Arıkan Özden.

Funding: The author(s) received no financial support for the research, authorship, and/or publication of this article.

References

[1] Ö. F. Sukas, Ö. K. Kınacı, and Ş. Bal, "Gemilerin manevra performans tahminleri için genel bir değerlendirme -I", *Gemi ve Deniz Teknolojisi,* vol. 23, pp.37-75, 2017.

[2] N. Groves, T. Huang, and M. Chang, "Geometric characteristics of DARPA SUBOFF models (DTRC Model Nos. 5470 and 5471)", 1989.

[3] R. Roddy, "Investigation of the stability and control characteristics of several configurations of the DARPA SUBOFF model (DTRC Model 5470) from captive- model experiments", 1990.

[4] T. Huang, and H. Liu, "Measurements of flows over an axisymmetric body with various appendages in a wind tunnel: the DARPA SUBOFF experimental program", 1994.

[5] "ITTC Manoeuvring Committee. (2014). Final report and recommendations to the 27th ITTC. Proceedings of the 27th International Towing Tank Conference, Copenhagen, Denmark."

[6] S. Toxopeus, and G. Vaz, "Calculation of current or manoeuvring forces using a viscous-flow solver". *International Conference on Offshore Mechanics and Arctic Engineering,* vol. 43451, pp. 717-728, 2009.

[7] G. Vaz, S. Toxopeus, and S. Holmes, "Calculation of manoeuvring forces on submarines using two viscous-flow solvers", *International Conference on Offshore Mechanics and Arctic Engineering,* vol. 49149, pp. 621-633, Dec 2010.

[8] S. Toxopeus, et al. "Collaborative CFD exercise for a submarine in a steady turn", *International Conference on Offshore Mechanics and Arctic Engineering,* vol. 44922, pp. 761-772, Aug 2012.

[9] Y. C. Pan, H. X. Zhang, and Q. D. Zhou, "Numerical prediction of submarine hydrodynamic coefficients using CFD simulation", *Journal of Hydrodynamics,* vol. 24, pp. 840-847, Dec 2012.

[10] A. Ray, and D. Sen, '"Identification of submarine hydrodynamic coefficients from sea trials using extended kalman filter", *10th International Conference on Hydrodynamics,* St. Petersburg, Russia, 2012.

[11] J. Jiang, Y. Shi, and G. Pan, "Computation of hydrodynamic coefficients of portable autonomous underwater vehicle", *Apcom Iscm*, pp. 1-6, 2013.

[12] A. Shadlaghani, and S. Mansoorzadeh, "Calculation of linear damping coefficients by numerical simulation of steady state experiments", *Journal of Applied Fluid Mechanics,* vol. 9, pp. 653-660, Feb 2016.

[13] Y. H. Lin, S. H. Tseng, and Y. H. Chen, "The experimental study on maneuvering derivatives of a submerged body SUBOFF by implementing the Planar Motion Mechanism tests", *Ocean Engineering,* vol. 170, pp. 120-135, Dec 2018.

[14] H. Atik, "Türbülans modellerinin DARPA SUBOFF statik sürükleme testi üzerinden incelenmesi", *Gazi Üniversitesi Mühendislik-Mimarlık Fakültesi Dergisi*, vol 3, pp. 1509-1522, 2021.

[15] E. Kahramanoglu, "Numerical investigation of the scale effect on the horizontal maneuvering derivatives of an underwater vehicle", *Ocean Engineering,* vol. 272, pp 113883, Mar 2023.

[16] H.L. Liu, and T. T. Huang, "Summary of DARPA suboff experimental program data," 1998.

[17] T. I. Fossen, "Guidance and control of ocean vehicles. Wiley," 1994.

[18] J. D. Mora Paz, and O. D. Tascón Muñoz, "Multiobjective optimization of a submarine hull design", *Ciencia y Tecnología de Buques*, vol. 7, pp. 27-42, 2014.

[19] M. A. Abkowitz, "Lectures on ship hydrodynamics – Steering and maneuvering", *Hydro & Aerodynamic Laboratory,* 1964.

[20] H. Yoon, "Phase-averaged stereo-PIV flow field and force/moment/motion measurements for surface combatant in PMM maneuvers" *The University of Iowa*, 2009.

[21] T. Sname, "Nomenclature for treating the motion of a submerged body through a fluid" *Technical and Research Bulletin,* pp. 1950.

[22] ITTC Resistance Committee, "Uncertainty analysis in CFD Verification and validation methodology and procedures", *ITTC - Recomm Proced. Guidel*, pp. 1-13, 2017.